JOURNAL OF GUIDANCE, CONTROL, AND DYNAMICS
Vol. 26, No. 5, September–October 2003

New Class of Optimal Plane Change Maneuvers

B. F. Villac* and D. J. Scheeres†
University of Michigan, Ann Arbor, Michigan 48109-2140

For planetary satellite orbiters (such as the Europa Orbiter Mission) and planet orbiters (such as the Mercury Messenger Mission), third-body forces can induce large changes in orbital elements over one orbit. As a result, transfers involving an ellipse cannot be considered without taking these forces into account, and two- and three-impulse transfers must model these effects at larger distances from the central body. A new use of third-body perturbations is presented to effect plane changes. It is shown, in particular, that large plane changes can be obtained by using only two impulsive maneuvers and a proper timing of the first burn. The resulting plane change maneuvers are shown to be optimal over classical one-impulse maneuvers for large enough inclination change values, replacing the classical optimality of bielliptic transfers (as compared to one-impulse plane changes) in the case of environments perturbed by a large, third body. The investigation is performed by solving an optimization problem with constraints and using the Hill three-body problem to describe the underlying dynamics. Savings on the order of 25% are obtained when compared to the one-impulse transfers for plane changes of ∼60 deg, and plane changes of ±180 deg are shown to be possible without escaping.

Introduction

PLANETARY satellite orbiter missions, such as the Europa Orbiter Mission, present new challenges to the design of trajectories, due to the large third-body perturbations that exist there. These disturbing forces represent the combined effect of the gravitational attraction of a large, perturbing body on the spacecraft, for example, Jupiter in the case of an Europa orbiter, and the motion of the central body due to this perturbing, third body.

It has been shown that for most planetary satellites in the solar system,[1] these disturbing forces can cause instabilities that result in the impact of the orbiter on the satellite over relatively short time spans, even for low-altitude trajectories. In particular, whereas low-inclination, circular orbits are stable, scientifically interesting orbits, such as near polar orbits needed for high-latitude mapping of the satellite, are unstable.[1−3] When a spacecraft is assumed to be in such an unstable trajectory, large plane change maneuvers may then be required to transfer it into a lower inclination, stable orbit to avoid impact with the satellite over long time spans. The classical results for plane change maneuvers, based on the two-body problem, assume no change in orbital elements during a transfer trajectory, and thus, are not applicable to these environments. Hence, the costs of the corresponding maneuvers predicted by these analyses are not representative of the physical situation.

As shown in a previous paper,[4] the effects of the third-body perturbations on a transfer trajectory are strongly dependent on the orbit orientation with respect to the perturbing body, which allows us to use the longitude of the ascending node Ω and the argument of periapsis ω to control these effects. These variables allow us to use the third-body perturbations as control forces for the design of transfer maneuvers, which results in lower costs and new optimal criteria for these maneuvers. Even though these effects hold for any transfers that involve raising the apoapsis radius, in this paper we focus on the case of plane change maneuvers. These transfers can be viewed as classic bielliptic plane changes with the apoapsis maneuver suppressed by the use of the third-body forces and represent the first step in extending the classical result on plane change maneuvers to the case of third-body perturbed environments.

The first section introduces the Hill[5] problem, which is a good model for the dynamics of particles in the environment of a planetary satellite (or even a sun–planet system) and present attractive analytical features that simplify the analysis (symmetries and nondimensional form). The characteristics of the dynamics close to the central body and on the transfer trajectory are also presented, showing the possibility of third-body-driven transfers. The next section focuses on the plane change maneuvers. It is shown that the numerical computation of such transfers involves the choice of precise values of the longitude of the ascending node relative to the satellite–planet line Ω and the argument of periapsis ω, which are obtained by solving an optimization problem over a Poincaré section. Then, a first analysis of their main characteristics is performed, showing, in particular, that third-body-driven plane changes can be less costly than one-impulse plane change maneuvers. A discussion on the limitations and extensions of these third-body-driven plane changes is finally given.

Third-Body-Driven Transfers and Dynamics in the Hill Model

Classically, the design of orbit transfers is based on the two-body problem for the underlying dynamics. In this model, the trajectory of a spacecraft is entirely determined by its five orbital elements, semimajor axis a, eccentricity e, inclination i, longitude of the ascending node Ω, and argument of periapsis ω until the next maneuver. In this situation, relations between two points on a given orbit are readily obtained, and the problem of determining a transfer can be viewed as a geometrical problem of the intersection of conics together with an optimization over all possible impulsive maneuvers. In particular, there is no distinction between the dynamics on the initial, final, and transfer orbits. The time appears as a secondary variable (possibly as a cost function) in the sense that, if a transfer is possible at time t_0, it is also possible at time $t_0 + T$, where T represents the period of motion on the initial orbit. Also, the absolute position of the initial and final orbits relative to a given inertial frame are not generally taken into account in the formulation of the problem, only the relative orientation of the initial orbit with respect to the final one is important. A typical example of transfer is given by the bielliptic plane change (or restricted three-impulse plane change[6]), where a spacecraft starts in an initial low-altitude, circular orbit, a first maneuver transfers it to an ellipse where a second maneuver is performed at apoapsis, changing its orbital plane, and a final

Presented as Paper 2002-4724 at the AIAA/AAS Astrodynamics Specialist Conference, Monterey, CA, 6 August 2002; received 4 October 2002; revision received 7 April 2003; accepted for publication 8 April 2003.

*Ph.D. Candidate, Aerospace Engineering; bvillac@umich.edu. Student Member AIAA.

†Associate Professor, Aerospace Engineering; scheeres@umich.edu. Senior Member AIAA.

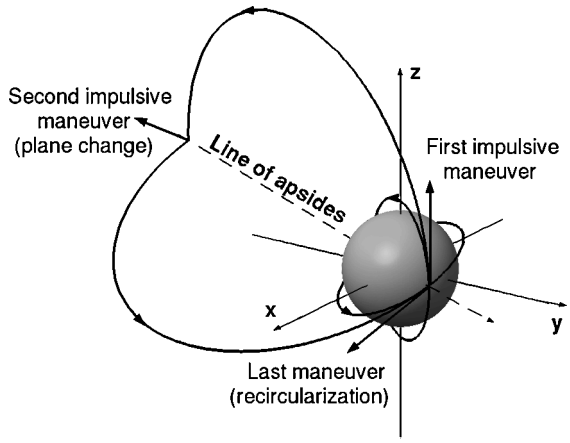

Fig. 1 Geometry of bielliptic plane changes.

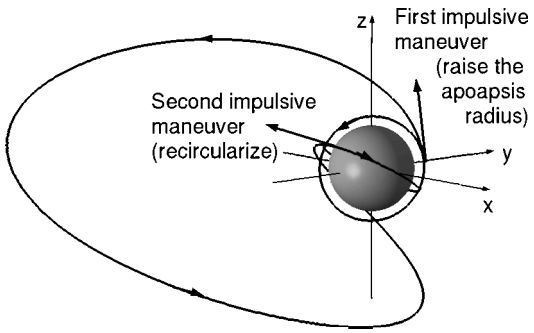

Fig. 2 Geometry of third-body-driven plane changes.

maneuver at the next periapsis retransfers the spacecraft to a low-altitude, circular orbit (Fig. 1).

When perturbations occur, however, this state of affairs changes. Orbital elements are now a function of time, and there may be no definite analytical relationship between two points on a given orbit. The situation is not so bad for small perturbations where averaging theory gives a good approximation of the secular changes of the orbital elements over one orbit. Because, by assumption, these perturbations are small, variations over one orbit remain small, and the two-body approximation retains its value and gives useful estimates of the ΔV required for a given maneuver. This is, for example, the case for orbiters moving in a J_2 perturbed gravitational field. Moreover, in this case, the perturbations decrease as the apoapsis of the transfer orbit is raised, which again justifies the two-body assumption. Still, even in this slightly perturbed environment, ω and Ω are shifted during each orbit, and the absolute orientation of the initial and final orbit at a given epoch enters into the problem.

As opposed to the J_2 perturbations, third-body forces become more prominent as one gets farther from the attracting body. Dynamics close to the satellite and on the transfer orbits now have very different characteristics, and the orientation of the initial and final orbits (or, equivalently, the timing of the maneuvers) is of prime importance. More precisely, when it is assumed that a spacecraft is in a low-altitude, circular orbit and that a ΔV maneuver is performed to place the spacecraft onto an eccentric orbit, performing the maneuver at time t_0 or $t_0 + T$ may result in an impact or escape from the satellite before the spacecraft has reached the next periapsis.[4] The initial value of ω and Ω now control, in some way, the changes that occur during a transfer orbit, and a careful choice of these variables allows us to use the third forces to generate the plane change without any cost (Fig. 2).

After presenting the model used to characterize the third-body effects in the next subsection, the assumptions and dynamics that make such transfers possible are presented.

Table 1 Physical parameters for Mercury, Earth, Europa, Titan, and Triton[7]

Primary body (perturbing body)	Length scale, km	Timescale, h	Normalized radius
Mercury (sun)	318,272	336.00	0.007
Earth (sun)	2,158,322	1,395.09	0.0029
Europa (Jupiter)	19,692	13.56	0.079
Titan (Saturn)	1,214	5.39	0.199
Triton (Neptune)	38,406	22.44	0.045

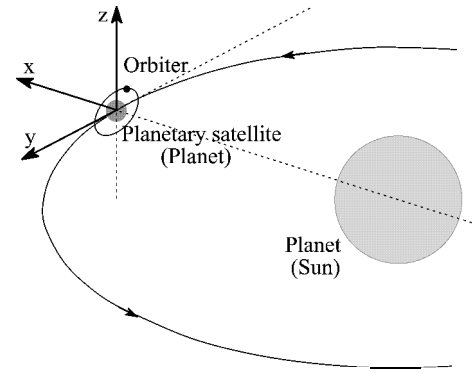

Fig. 3 Geometry of the Hill problem.

Hill Model

This model was first derived by Hill[5] to explain the motion of the moon around the Earth and is a useful model to characterize the motion of two close masses perturbed by a larger, massive object. In particular, this model describes the dynamics of a spacecraft in the environment of a planetary satellite, or even in a large orbit about a planet.

This model is given by the following set of differential equations:

$$\ddot{x} - 2N\dot{y} = -(\mu/r^3)x + 3N^2x \tag{1}$$

$$\ddot{y} + 2N\dot{x} = -(\mu/r^3)y \tag{2}$$

$$\ddot{z} = -(\mu/r^3)z - N^2z \tag{3}$$

where (x, y, z) are the Cartesian coordinates of a rotating frame (Fig. 3), $r = \sqrt{(x^2 + y^2 + z^2)}$ is the magnitude of the radius vector, N is the angular velocity of the satellite (planet) around the planet (sun), and μ is its gravitational parameter.

These equations can be made nondimensional and parameterless by setting the length and timescales to be $l = (\mu/N^2)^{1/3}$ and $\tau = 1/N$, respectively. The resulting equations are obtained by setting $\mu = 1$ and $N = 1$ in the preceding set of equations. Therefore, all of the analysis performed on the nondimensional system can be scaled to any physical system by setting the proper length scale and timescale. This feature makes the Hill model an attractive dynamic model for preliminary studies, and all of the computations presented in this paper are performed in this normalized setting. Table 1 gives the length and timescales of a few planetary satellites of the solar system and of Mercury and the Earth (as perturbed by the sun) (see Ref. 7).

Dynamics Close to the Primary

Note that l and τ give the length scale and timescale at which the non-Keplerian phenomena of the dynamics become important. For instance, the libration points L_1 and L_2 are situated on the x axis at a distance of $(\frac{1}{3})^{1/3}l \simeq 0.69l$ from the center of mass, and $2\pi\tau$ is the period of motion of the satellite (planet) around the massive planet (sun). This shows that for small values of radius and short timescales (as compared to l and τ), the dynamics become close to Keplerian and the motion is only slightly disturbed. This is in accordance with our physical intuition of a tightly bound trajectory or the notion of a sphere of influence in interplanetary trajectories. (The disturbing planet is far away and its gravitational pull is small

when compared to the primary.) Note also that for $N = 0$ the Hill model reduces to the two-body problem.

In such a realm of motion, third-body perturbations can be averaged over as has been done by Scheeres et al.[1] More precisely, a double time averaging has been performed because one order of magnitude appears between the mean motion of the spacecraft around the satellite and the mean motion of the satellite around the planet, when the motion is considered for low-altitude, nearly circular orbits of normalized radius less than 0.215. The results of the analysis show that, even though the third-body perturbations are small, they can generate instabilities that can cause a spacecraft to impact the surface of the satellite after a few weeks or months for the case of Europa. These instabilities appear only for certain ranges of the inclination (near polar orbits, $39.23 < i < 140.77$ deg) and are characterized by an exponential growth of the eccentricity. However, the timescale for such an exponential growth is large when compared to the orbital motion of the spacecraft and is an order of magnitude larger than the period of Europa about the planet. The semimajor axis and inclination remain constant on average (at first order in e), which means that, starting from an initial quasi-circular orbit of eccentricity 0.001, the eccentricity will be less than 0.01 for a number of revolutions of Europa around the planet. In other words, with regard to orbital transfer maneuvers, one can assume that a spacecraft is in a low-altitude, circular orbit with a precessing ascending node relative to the satellite–planet (planet–sun) line. That is, $\Omega = \Omega_0 - Nt$ and $M = M_0 + nt$, where Ω and M are the longitude of the ascending node relative to the x axis (rotating frame) and the mean anomaly, respectively. The quantity $n = \sqrt{(\mu/r_0)}$ is the mean motion of the spacecraft on the circular orbit of radius r_0. Hence, the trajectory of a spacecraft on a low-altitude, circular orbit can be pictured as a line wrapping on the (M, Ω)-torus space (Fig. 4).

Table 2 gives some characteristics of these instabilities (based on the results obtained by Scheeres et al.[1]) for the few celestial bodies in Table 1, together with a bound on the positioning error for ω and Ω for a time span of one satellite period. More precisely, the characteristic instability time τ_S represents the inverse of the exponential characteristic of the eccentricity growth [$e(t) \simeq \exp(\lambda t)$ and $\tau_S = 1/\lambda$] for a polar orbit. The eccentricity will grow by an order of magnitude after $\ell n(10) \simeq 2.302, \ldots,$ characteristic times. Finally, when it is assumed that the mean motion of the spacecraft is n and the mean motion of the primary is N, the simple rotation of the frame implies that, given some nominal value Ω_0 of the longitude of the ascending node, the spacecraft can reach any value of mean anomaly within one revolution around the primary and a shift in Ω by $\pm 180\, N/n$ (positioning error on Ω). Note that this positional accuracy will improve orbit after orbit.

Table 2 Parameters for the dynamics close to Mercury, Earth, Europa, Titan, and Triton[1]

Primary	Characteristic instability time τ_S	Mean motion ratio, N/n	Positioning error on Ω, deg
Mercury	>30 years	0.00067	0.12
Earth	>500 years	0.00016	0.029
Europa	13.66 days	0.0225	4.05
Titan	220.28 days	0.00627	1.12
Triton	31.20 days	0.0163	2.93

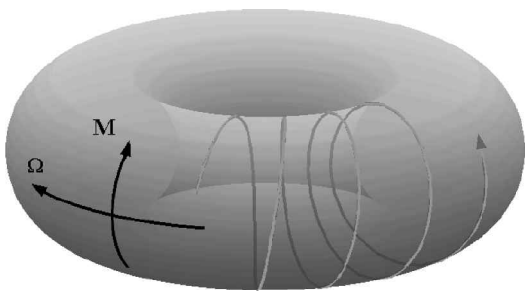

Fig. 4 Representation of the motion on a low-altitude, circular orbit.

Outside this instability region, the eccentricity is shown to oscillate around its initial value and, once again, one can assume the spacecraft to be in a circular orbit over a number of orbits. These assumptions are by no means necessary for the practical application of the transfers described later, but ease the understanding of the geometry of the maneuver and the comparisons to be made.

Orbital Dynamics

As mentioned earlier, the idea of our third-body-driven transfers is to place the spacecraft into a highly eccentric transfer trajectory (to raise the apoapsis radius) so that the large third-body forces can perform plane change maneuvers without any ΔV costs at apoapsis. This implies that the spacecraft will start from one periapsis and follow the transfer trajectory to the next periapsis (Fig. 2). Such motion is then fully characterized by the change in orbital elements from one periapsis to the next one. These orbital dynamics are, in spirit, the same as a Poincaré section used to investigate the dynamics close to a periodic orbit. Here, the sections are defined by the periapsis condition $\dot{r} = 0$ and $\ddot{r} > 0$.

These conditions define a five-dimensional manifold in the phase space of the system that is transversal to the flow for periapsis smaller than 0.2 in the Hill problem (which contains the domain of phase space in which we are interested: low-altitude, initial and final circular orbits).

The initial phase space is furthermore restricted by assuming that the spacecraft is in an initially circular orbit with a given semimajor axis and inclination and that the ΔV of the first maneuver is fixed (or, equivalently, that the apoapsis radius of the transfer trajectory is fixed at periapsis). The only remaining variables are then the argument of periapsis and the longitude of the ascending node, parameterizing the surface of a torus.

The flow can then be integrated numerically to obtain a map of the dynamics from one periapsis to the next. Figure 5 gives an example of such a computation showing the change in periapsis radius Δr_p and inclination Δi over one iteration of the map. Note that the values of ω and Ω at the next crossing are different from the initial values in general.

These contour plots strongly indicate a symmetry in ω and Ω. This is indeed the case, and one can check that the Hill equations of motion are invariant under several transformations, generated by three independent symmetries S_1, S_2, and S_3. If $(x, y, z, \dot{x}, \dot{y}, \dot{z}, t)$ denotes a solution of the equations of motion, then the trajectories obtained by applying the following transformations are also valid solutions:

$$(x, y, z, \dot{x}, \dot{y}, \dot{z}, t) \xrightarrow{S_1} (-x, y, z, \dot{x}, -\dot{y}, -\dot{z}, -t)$$

$$(x, y, z, \dot{x}, \dot{y}, \dot{z}, t) \xrightarrow{S_2} (x, -y, z, -\dot{x}, \dot{y}, -\dot{z}, -t)$$

$$(x, y, z, \dot{x}, \dot{y}, \dot{z}, t) \xrightarrow{S_3} (x, y, -z, \dot{x}, \dot{y}, -\dot{z}, t)$$

The composition of these three symmetries yield other symmetries; notably the composition of Eqs. (1) and (2) yields

$$(x, y, z, \dot{x}, \dot{y}, \dot{z}, t) \xrightarrow{S_4} (-x, -y, z, -\dot{x}, -\dot{y}, \dot{z}, t)$$

This last symmetry corresponds to a symmetry about the origin in the (x, y) plane, which is equivalent to a symmetry of motion for shifts in ω of the form $\omega + m\pi$, $m = 0, \pm 1, \ldots$. Also the S_3 symmetry [reflection about the (x, y) plane] is equivalent to a symmetry in Ω of the form $\Omega \to \Omega + m\pi$.

Therefore, all of the dynamics of the transfer trajectories can be represented on the region $[0, 180] \times [0, 180]$ deg of the (ω, Ω) space.

Another interesting feature of Fig. 5 is the presence of zero lines. That is, there exist some values of argument of periapsis and longitude of the ascending node for which the change of periapsis radius from one periapsis to the next one is zero. This is precisely one of the ingredients needed for the case of a plane change transfer.

As apoapsis is raised, that is, the initial ΔV is incremented, third-body perturbations become stronger and can cause the spacecraft

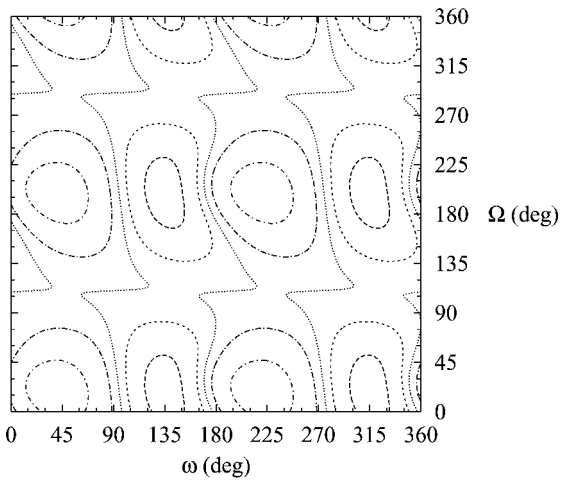

a)

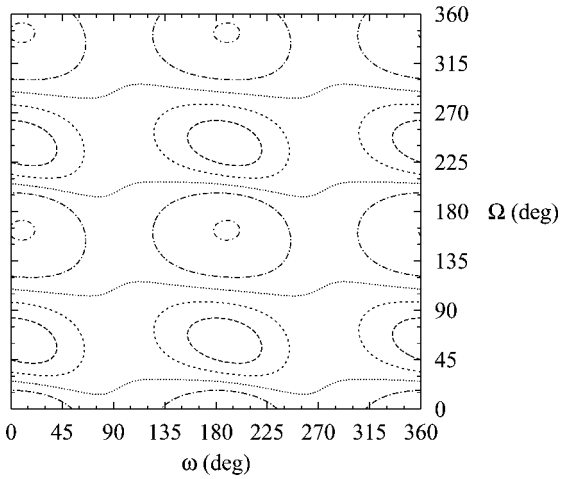

b)

Fig. 5 Contour plots for Δr_p and Δi with $r_p = 0.08$, $r_a = 0.4$, and $i = 90$ deg; a) change in periapsis radius: - - - -, $\Delta r_p = 0.03$; ▪▪▪▪, $\Delta r_p = 0.01$; · · · ·, $\Delta r_p = 0$; ------, $\Delta r_p = -0.01$; and -▪-▪-▪, $\Delta r_p = -0.03$ and b) change in inclination, degree: - - - -, $\Delta i = 10$; ▪▪▪▪, $\Delta i = 5$; ...., $\Delta i = 0$; ------, $\Delta i = -5$; and -▪-▪-▪, $\Delta i = -15$.

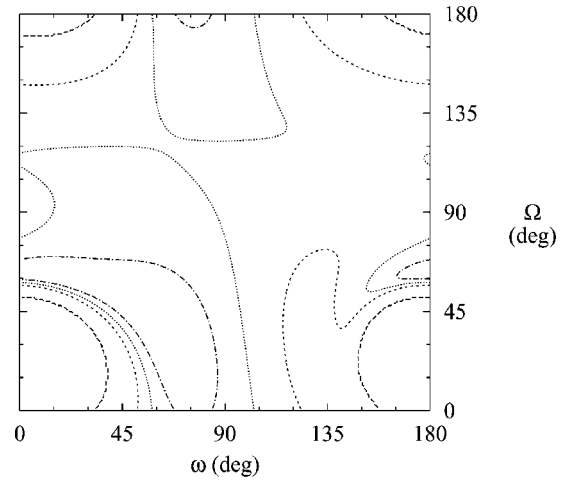

a)

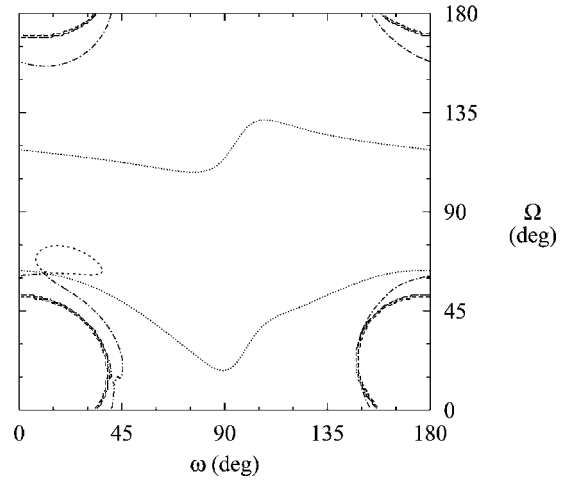

b)

Fig. 6 Contour plots for Δr_p and Δi with $r_p = 0.08$, $r_a = 0.6$, and $i = 90$ deg where contours with value +1e05 delineate the escape regions; a) change in periapsis radius: - - - -, $\Delta r_p = 1e+05$; ▪▪▪▪, $\Delta r_p = 0.1$; · · · ·, $\Delta r_p = 0$; and ------, $\Delta r_p = -0.05$ and b) change in inclination, degree: - - - -, $\Delta i = 1e+05$; ▪▪▪▪, $\Delta i = 45$; · · · ·, $\Delta i = 0$; and ------, $\Delta i = -50$.

to escape from the planetary satellite (planet). Figure 6 shows two examples of such contour plots with escape regions. Notice that the topology of the zero curves has changed. There is now only one zero curve, and it does not fill the whole Ω space. This means that there are some time spans over which no transfer maneuvers can be performed, whatever the value of ω. However, the $\Delta r_p = 0$ lines still cross the axes $\omega = 0$ deg and $\Omega = 20$ deg transversally. The point ($\omega = 0$, $\Omega = 20$ deg) represents the approximate values of the argument of periapsis and longitude of the ascending node of the periapsis of the stable manifold associated with the libration point L_1 and corresponds to the center of sets of periapsis of escaping trajectories (see Villac and Scheeres[8]). Neighborhoods of these sets present strong variations in Δr_p, and one can think of the lines $\omega = 0$ deg and $\Omega = 20$ deg as representing two principal directions along which variations in orbital elements are stronger. As a consequence, one can expect that the $\Delta r_p = 0$ lines will meet one or the other axis at some point.

Also observe that, as the inclination changes from 0 to 180 deg, the orbital element changes over one orbit get larger around 90 deg and, at the same time, the homotopy type of the zero curves changes. These transitions reflect that, for $i = 0$ deg, the dynamics depend solely on $\omega + \Omega$, whereas at $i = 180$ deg they only depend on $\omega - \Omega$. This corresponds to a rotation by 90 deg of the overall features of the contour plots and, notably, of the zero lines.

Finally, one can see in Fig. 6 that the values of ω and Ω have a very strong influence on the dynamics of the transfer orbits, as was already noticed.[4] A change by a few tens of degrees in one of these variables can lead to an escape or impact, all other elements remaining equal.

Third-Body-Driven Plane Changes

In the preceding section, we have shown that third-body perturbations can produce large changes in orbital elements over a single orbit and that these forces can be "controlled" by choosing ω and Ω of the transfer orbit. In this section, we specialize the analysis to plane change maneuvers where the criterion to be met is a zero change in periapsis radius while achieving a maximum plane change over a single transfer trajectory. Inspection of the Fig. 5 and 6 contour plots indicates the possibility of such transfers in conjunction with large changes in inclination.

After briefly reviewing the geometry of the plane change maneuvers analyzed in this paper, a numerical exploration of the possibilities of such transfers is discussed. Maximum plane changes as a function of apoapsis radius are obtained by solving an optimization problem under the constraint $\Delta r_p = 0$, and comparisons with the classical one-impulse maneuvers are given.

Geometry of the Transfers

As noted in the Introduction, the third-body-drivenplane changes considered are analogous to bielliptic plane changes, with the

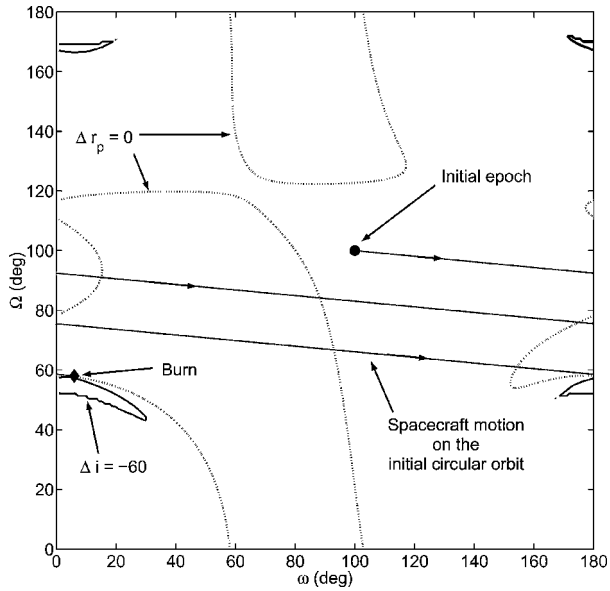

Fig. 7 Timing of the first burn.

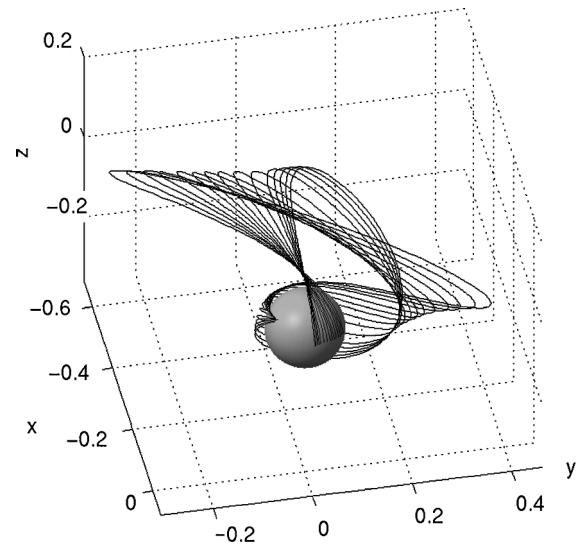

Fig. 8 Series of third-body-driven plane changes for the Europa case, $r_p = 0.08$, $i = 90$ deg, with plane changes range from −40 to −60.

apoapsis maneuver replaced by the "cost free" action of the third-body perturbations. More precisely, consider a spacecraft initially in a low-altitude, circular orbit. A first tangential burn places the spacecraft into a highly eccentric orbit. This first maneuver determines the elements of the transfer trajectory at periapsis. In particular, the argument of periapsis and the longitude of the ascending node are directly determined by the time at which the maneuver is performed. One can view the spacecraft moving on its initial circular orbit as describing a line (parameterized by time) on the (ω, Ω)-torus space of the Figs. 5 and 6 contour plots. The value of ω and Ω at a point of this line would correspond to the value of the argument of periapsis and longitude of the ascending node of the transfer trajectory if the maneuver were performed at that point (Ω being measured with respect to the x-axis that is, the planet–satellite or sun–planet line, at the time of the maneuver). That is, on the initial circular orbit, one makes the association $M \sim nt \leftrightarrow \omega$ and $\Omega \sim -Nt \leftrightarrow \Omega$. Figure 7 illustrates such an association. The $\Delta r_p = 0$ lines are represented together with the trajectory of the spacecraft on the initial circular orbit as viewed in the (ω, Ω)-torus space. The burn of the first maneuver is performed when the targeted values of ω and Ω are met. As noticed earlier ("Dynamics Close to the Primary" subsection), proper timing of the maneuver allows us to choose these values with a fair accuracy.

After this first maneuver, the third-body forces cause changes in the orbital elements as the spacecraft completes one orbit. At the next periapsis, a plane change has occurred while the careful choice of ω and Ω ensured that no net change in periapsis radius occurred. A second tangential maneuver is then used to place the spacecraft in its final, low-altitude circular orbit (Fig. 2). Because of changes in semimajor axis and eccentricity during the transfer, the magnitude of this recircularizing burn is not, in general, equal to the magnitude of the first maneuver.

Figure 8 presents a series of numerically integrated transfer trajectories for plane changes ranging from −40 to −60 deg in the case of an Europa orbiter. It is clearly seen that the initial values of Ω vary as the desired value of the inclination change is varied. This is to be expected because ω and Ω are used as control variables, and their values are fixed by the amount of plane change to be performed. Moreover, their values at the next periapsis are also fixed, which shows the lack of direct control of the longitude of the ascending node on the final orbit. However, because Ω precesses in this environment, phasing methods can be used to achieve specific values of Ω_0 at a given epoch.

Numerical Solution for Maximum and Minimum Plane Change

The preceding discussion shows that third-body-driven plane changes can be computed by solving an optimization problem over the Poincaré sections defined by the periapsis conditions. More precisely, the values of ω and Ω that yield a desired plane change are computed by solving the maximum and minimum values of plane change realizable for a given value of initial inclination, periapsis, and apoapsis radii, that is, ΔV. That is, we solve the following nonconvex optimization problem:

$$(\omega, \Omega) = \arg\max_{\omega,\Omega} \left\{ \Delta i_{(\omega,\Omega)} | \Delta r_{p_{(\omega,\Omega)}} = 0 \right\} \tag{4}$$

respectively, $\arg\min\{\Delta i | \Delta r_p = 0\}$ for the minimum plane change. Even though this problem can a priori be solved by standard optimization algorithms, the numerical procedure used here consists of first searching the Δr_p zero lines on the torus $[0, 180] \times [0, 180]$ deg and then looking for the maximum plane change on these zero lines. This method has the advantage of not necessitating an initial guess while allowing us to keep track of the zero lines.

The search for the $\Delta r_p = 0$ lines is performed by first searching the crossings of the lines with the axes $\omega = 0$ deg and $\Omega = 20$ deg and then tracking the zero lines from these points. As explained in the subsection "Orbital Dynamics," the choice of these search axes has been determined using both physical reasoning and numerical exploration of several contour plots (such as the ones given in Figs. 5 and 6). It is assumed that the number of crossings on one axis does not exceed 10, but in all of the cases considered, a maximum of 4 crossings and a minimum of 2 has been found. The search for the crossings is performed by setting a uniform grid on each axis and looking for a change of sign between two consecutive nodes. The step size used is 0.1 deg, so that two different zero lines are assumed to be separated by at least such a value. This also implies that the escape regions must not lie within 0.1 deg of a zero line.

Note that these assumptions do not allow us to conclude that the extrema found are global, but it avoids a blind search of the entire (ω, Ω) space. (We may miss a zero line.) Also, when such a global search has been performed, the results obtained agreed with the results returned by the preceding algorithm.

After this first search, the zero lines are tracked by moving, step by step, along the tangent of these zero lines. [The tangent vector to a zero line is given by $(\partial \Delta r_p / \partial \Omega, -\partial \Delta r_p / \partial \omega)$. These partial derivatives can be either computed by a finite difference scheme or by computing the state transition matrix of the Hill problem and transforming the results into orbital elements.] Again it is assumed that no escape region lies within 5.7×10^{-3} deg of these lines, which has always been the case in the domain of phase space considered. However, for large enough apoapsis radius, this may not be the case, and the neighborhoods of the escape regions present very strong variations in orbital elements that cannot be computed with the

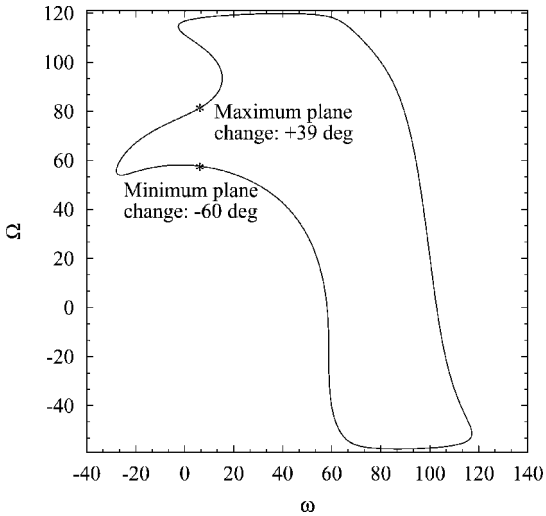

Fig. 9 $\Delta r_p = 0$ lines for $r_p = 0.08$, $r_a = 0.6$, and $i = 90$ deg.

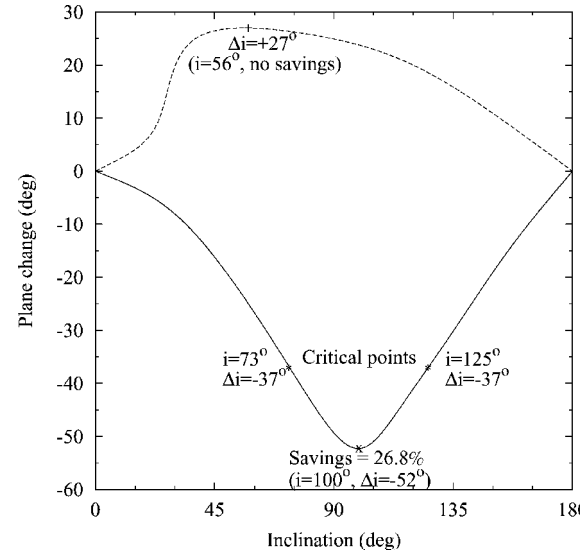

Fig. 10 Extrema values of plane change as a function of inclination, $r_p = 0.08$ and $r_a = 0.5$.

preceding assumptions. The maximum step size used to perform this tracking is 1 deg, and a search for the maximum and minimum Δi is then performed over all of these points. This means that the determination of the global maximum of plane change is performed to within this limit.

Once the maximum (or minimum) has been found, the accuracy is improved up to 5.7×10^{-3} deg, that is, the positional accuracy of the local maximum is 5.7×10^{-3} deg. Note that all integrations performed use a Runge–Kutta–Felhberg integrator of order 7–8, with an accuracy of 10^{-10} (per step).

Figure 9 gives an example of such a computation where the zero lines have been computed for the same initial values as in Fig. 6. The position of the maximum and minimum of plane change is indicated.

Finally, note that the dynamics considered here are smooth (or, at least, continuous), so that when the maximum and minimum plane changes are located on the same Δr_p zero line, all values of plane change between these two extrema are possible. For the case in Fig. 9, we see that plane changes between $+39$ and -60 deg are possible by timing the initial impulsive maneuver. For other cases, such as ± 180-deg plane changes indicated in the next subsection, the maximum and minimum plane changes are located on two different, separated zero lines, and not all of the values of plane change between these extrema are realizable.

Variations with Initial Elements

Once this computation has been performed for a given set of values of periapsis radius, apoapsis radius, and inclination, the algorithm is repeated to cover a wide range of cases. Figures 10–14 give the results of such computations when the initial inclination, apoapsis radius, and periapsis radius, respectively, are varied. Figures 10–14 each have been computed with at least 90 points for the independent variable.

Variations with Initial Inclination

Two distinct behaviors of the variations of the minimum plane change are obtained when inclination varies, according to the initial values of periapsis radius r_p and apoapsis radius r_a.

For the lower values of apoapsis radius (at fixed r_p), the minimum and maximum plane changes obtained for the inclinations of 0 and 180 deg are zero. In this case, the changes in orbital elements become larger around an inclination of 90 deg, as can be seen in Fig. 10 for the change in inclination.

For higher values of apoapsis radius (or lower values of periapsis radius with fixed r_a), a bifurcation occurs, so that, at the inclinations of 0 and 180 deg, a maximum and minimum plane change of 180 and -180 deg, respectively, are obtained, as can be seen in Fig. 11 and 12. [Only plane changes of -180 deg are possible with the initial conditions chosen for Fig. 11. Plane changes of 180 deg are possible for higher apoapsis radii, for example, $r_a = 0.8$, but some zero lines

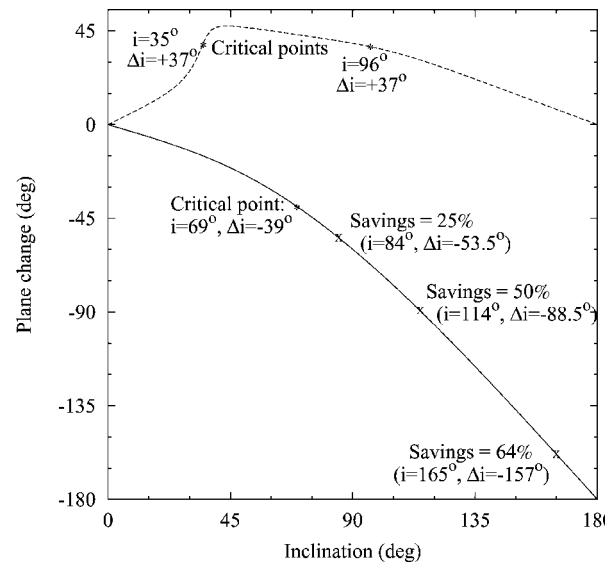

Fig. 11 Extrema values of plane change as a function of inclination, $r_p = 0.08$ and $r_a = 0.6$.

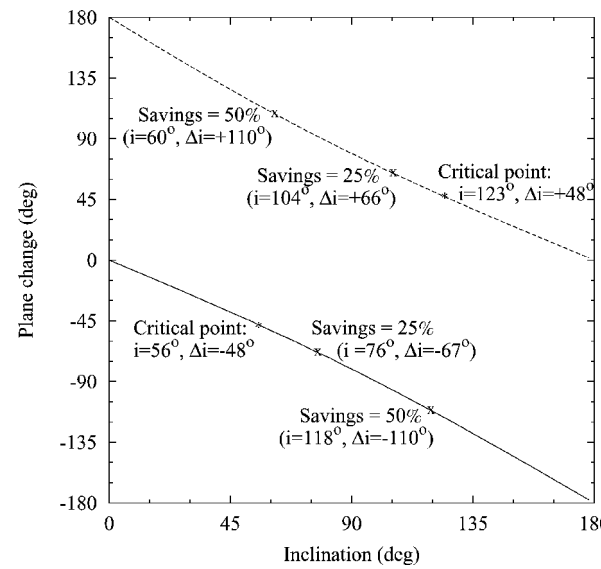

Fig. 12 Extrema values of plane change as a function of inclination, $r_p = 0.003$ and $r_a = 0.5$.

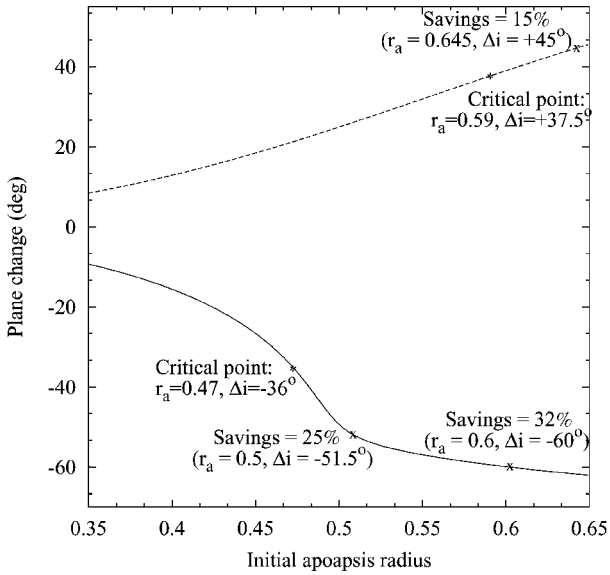

Fig. 13 Extrema values of plane change as a function of apoapsis radius, $r_p = 0.08$ and $i = 90$ deg.

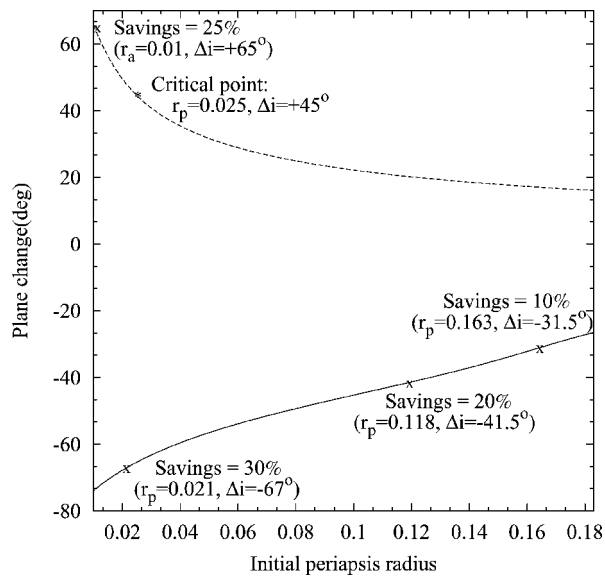

Fig. 14 Extrema values of plane change as a function of periapsis radius, $r_a = 0.5$ and $i = 90$ deg.

cannot be computed at such a high value of r_a with the present program.] Note that this result is consistent with the invariance of the (x, y) plane in the Hill model. A plane change of ± 180 deg at an inclination of 0 or 180 deg corresponds, indeed, to a change in the direction of motion relative to the primary (change from retrograde to prograde orbit or vice versa) and does not involve any z component of the velocity vector. The motion remains planar during such a transfer.

Figures 10–12 also show that the bifurcations for positive and negative plane changes do not necessarily occur for the same values of periapsis and apoapsis radii. The few numerical explorations performed suggest that the bifurcation for negative plane changes occurs at lower values of apoapsis radius than that for positive plane changes. In fact, as clearly appears in Figs. 10–14, the dynamics are not symmetric for positive and negative plane changes, even though there are some similarities. It seems that, at any value of r_p and r_a, the overall maximum plane change realizable, that is, over all initial inclinations, is less than the overall negative plane change possible (in absolute value).

In the rest of this subsection, an inclination of 90 deg has been assumed as a representative initial inclination for the study of the variations of plane change with apoapsis radius and periapsis radius. Such an inclination corresponds, indeed, to the mean inclination over the unstable region for planetary satellite orbiters (see subsection "Dynamics Close to the Primary") and gives a good representation of the dynamics considered.

Variations with Initial Apoapsis Radius

As the initial apoapsis radius is raised, the plane changes obtained become larger, as expected (Fig. 13). Here again, the dynamics are not symmetric for the maximum and minimum plane changes; positive plane changes remain smaller than the negative plane changes. However, in both cases, large plane changes can be obtained, and for initial apoapsis radius larger than 0.7 (with $r_p = 0.08$ and $i = 90$ deg), both positive and negative plane changes allow us to transfer an unstable polar orbiter back to a stable region over a single transfer trajectory. For such values of apoapsis radius, both positive and negative plane changes are, indeed, larger than 50 deg.

Variations with Initial Periapsis Radius

At fixed apoapsis radius, a decrease in the initial periapsis radius results in the amplification of the third-body effects. As a consequence, larger plane changes can be obtained, as shown in Fig. 14 Note that, even though the Hill problem has a similarity property, that is, it can be made nondimensional so that each system modeled by the Hill equations of motion can be mapped into one another by a simple scaling, it is not true that the dynamics are similar at different values of the normalized radius. In particular, an increase in r_p with a fixed ratio r_p/r_a does not mean that the plane changes realizable are the same. For instance, at $r_p = 0.08$ and $r_a = 0.4$, the minimum plane change is smaller (in absolute value) than -20 deg, whereas for $r_p = 0.1$ and $r_a = 0.5$, the minimum plane change achievable is larger than -40 deg. That is, as the periapsis radius increases with fixed r_p/r_a ratio, the extrema of plane change achievable increase. These dynamics are also not linear in the sense that they do not depend solely on the difference between r_a and r_p, as can be easily checked in Figs. 13 and 14.

Finally, notice that third-body-driven plane changes of more than 60 deg (both positive and negative) are possible, hence, realizing inclination change values that would classically be performed using parabolic transfers.

Comparison with Classical Transfers and Optimality

Comparison Scales

Classical results[6] on plane change maneuvers indicate that the general three-impulse plane change maneuvers, that is, bielliptic transfers, as shown in Fig. 1, with additional small plane changes performed at the first and third burns) are always optimal over one-impulse and restricted bielliptic plane changes.

However, this transfer involves raising the apoapsis radius and, as was noted in the Introduction, this cannot be done in strongly perturbed environments without taking into account the perturbations. Therefore, only the one impulse classic result is still applicable in such environments and, hence, represents the only classic approach to be compared to third-body driven plane changes. The ΔV cost required to perform such a maneuver is given by

$$\Delta V_0 = 2V_{lc} \sin(\Delta i/2) \tag{5}$$

where $V_{lc} = \sqrt{(1/r)}$ is the local circular speed at the time of the maneuver.

Note that this cost decreases as we get farther from the attracting body and that classically, restricted bielliptic transfers become less costly for changes in inclination Δi greater than ~ 39 deg. For plane changes larger than 60 deg, the optimal classic approach (even when compared to the full three-impulse plane change maneuvers) is to perform a parabolic plane change maneuver, that is, a bielliptic transfer with the apoapsis radius raised to infinity. In such a case, the total ΔV is given by

$$\Delta V = 2V_{lc}\left[\sqrt{2} - 1\right] \tag{6}$$

Even if these transfers are not applicable in the environment considered, a few comparisons with these transfers are given in the text

to give an idea of the costs for performing large plane changes in third-body-perturbed environments. Parabolic transfers can indeed be considered as a standard scale to estimate the costs of large plane change maneuvers in preliminary mission analyses.

Note that this scale always corresponds to an overestimate of the costs for performing large plane changes in third-body-perturbed environments. Indeed, parabolic transfers involve the same number of burns as the third-body-driven plane change maneuvers, but their magnitude is always larger than in the third-body-driven case.

Numerical Results

The ΔV comparisons between the one impulse maneuver [Eq. (5)] and third-body-driven plane changes considered in this paper are given in Figs. 10–14. The tags shown in Figs. 10–14 indicate some values of the savings obtained when using third-body-driven plane changes. In particular, it is seen that savings larger than 25% are obtained for large plane change maneuvers ($\sim$60 deg).

The critical points also indicated in Figs. 10–14 show the values of the initial elements and plane change for which the transition of optimality between one impulse maneuvers and third-body-driven plane changes occurs. That is, for inclination changes larger than the critical values, third-body-driven plane changes are less costly than one-impulse maneuvers. These critical plane change values depend on the initial conditions of the low-altitude, circular orbit (r_p, r_a, and i) and seem to increase (in absolute value) as the periapsis radius decreases. For periapsis on the order of the normalized radius of Europa, the critical values for optimality lie close to 38 deg.

As expected, for plane changes larger than 60 deg, third-body-driven maneuvers are less costly than the classic scale of parabolic plane changes. The costs are lower by $\sim$5–10% in the case of Fig. 14 and more than 15% in the case of Fig. 13. Also, note the large savings made for the case of change of direction of motion (plane changes of -180 deg), as shown in Figs. 11 and 12. In this case, savings of more than 15% are obtained when compared to the parabolic transfers and more than 70% as compared to one-impulse plane changes. In addition, such transfers have the advantage of remaining bounded, and in particular, the transfer time is much smaller than in the parabolic case.

All of these results show that the classical optimality of bielliptic transfers over one-impulse maneuvers for plane changes larger than 39 deg has an analog in the case of third-body-perturbed environments, where bielliptic transfers are replaced by the third-body-driven plane changes defined here. This situation is, however, more complex than in the classical case because at any given initial conditions, the range of third-body-driven plane changes realizable is restricted. For example, the equatorial plane is invariant under the flow of the Hill equations, and the only plane changes possible are 0 or ± 180 deg. One cannot transfer a spacecraft from the equatorial plane to a polar orbit using only the natural dynamics, whereas it is perfectly possible to do this using a one-impulse maneuver. Further work will aim at characterizing the limits of optimality more fully.

Limitations and Extensions

The preceding limitation of only using the natural dynamics to perform the plane change could be removed by performing plane changes at the first and last burn. With the addition of an apoapsis maneuver, these transfers would generalize the classic full three-impulse plane change to the case of third-body-perturbed environments, improving the savings obtained here. This approach would unconditionally improve on the classical results. The analysis becomes much more involved, however, as the number of degrees of freedom increase.

Also, because the third-body-driven maneuvers involve raising the apoapsis radius to a significant distance from the central body, these transfers are not the cheapest solution when other celestial bodies are within these distance ranges. Flybys represent yet another use of the natural dynamic environment to reduce effectively the cost for performing orbital elements changes. This is the case in the Earth environment, where the moon can be used to perform large plane change maneuvers.

Finally, note that the results presented here can be modified to match the more general case of radius and plane change maneuvers. Instead of computing the zero lines of Δr_p, one has to compute the lines $\Delta r_p = \alpha$, where α represents the amount of desired radius change. Though larger savings may be possible in such cases, the order of magnitude of the savings obtained for the case $\Delta r_p = 0$ should be attainable because these zero lines correspond to a change of sign of the function $\Delta r_p(\omega, \Omega)$, so that performing the first maneuver a little ahead or after the values considered here should yield a positive or negative net change in periapsis radius while keeping the values of plane change realized with the zero periapsis change. This may be of interest for safety issues, where a decrease in periapsis radius is generally not desirable.

Conclusions

A new class of plane change maneuvers in environments perturbed by a third body has been presented. The use of the natural third-body forces allowed us to reduce the costs of plane change maneuvers by performing the desired plane change without using an impulsive maneuver during the transfer orbit. These new types of transfers (third-body-driven plane changes) are based on the idea of the classic bielliptic plane change with the apoapsis maneuver suppressed, resulting in a two-impulse plane change maneuver. Their implementation only involves timing of the first burn to approximate optimal values for the longitude of the ascending node (relative to the sun–planet line) and the argument of periapsis of the transfer ellipse. A numerical approach has been proposed to compute these optimal values.

It has been shown that the new plane change maneuvers can be less costly than one-impulse maneuvers and can represent a simple way of reducing the cost of plane change maneuvers when no flybys are possible. Savings on the order of 25% as compared with one-impulse maneuvers are obtained for plane changes of $\sim$60 deg, and the possibility of a reversal of the direction of motion (plane changes of ± 180 deg) has been shown to exist using such an approach. Savings of more than 15% when compared to the classic results on parabolic transfers and 70% when compared one-impulse maneuvers are realized in these cases.

Larger savings should be possible by considering a combination of both the classical methods and the approach outlined in this paper, that is, a strategy using the third-body forces and performing plane change maneuvers at each burn. Further investigations of the topology of the change in orbital elements over one- and-one-half orbits, however, seem necessary to be able to evaluate such an approach.

Acknowledgments

The work described was funded by the Interplanetary Network Directorate Technology Program and Outer Planets/Solar Probe Project by grants from the Jet Propulsion Laboratory, California Institute of Technology, which is under contract with NASA.

References

[1] Scheeres, D. J., Guman, M. D., and Villac, B. F., "Stability Analysis of Planetary Satellite Orbiters: Application to the Europa Orbiter," *Journal of Guidance, Control, and Dynamics*, Vol. 24, No. 4, 2001, pp. 778–780.

[2] Kozai, Y., "Motion of a Lunar Orbiter," *Publication of the Astronomical Society of Japan*, Vol. 15, No. 3, 1963, pp. 301–312.

[3] Conway, B., "Stability and Evolution of Primeval Lunar Satellite Orbiters," *Icarus, International Journal of the Solar System*, Vol. 66, No. 2, 1986, pp. 324–329.

[4] Villac, B. F., Scheeres, D. J., D'Amario, L. A., and Guman, M. D., "Effect of Tidal Forces in Orbit Transfers," *Proceedings of the AAS/AIAA Spaceflight Mechanics Meeting*, American Astronautical Society, Washington, DC, 2001, pp. 2049–2070.

[5] Hill, G. W., "Researches in the Lunar Theory," *American Journal of Mathematics*, Vol. 1, No. 1, 1878, pp. 5–26.

[6] Chobotov, V. A. (ed.), *Orbital Mechanics*, AIAA Education Series, 3rd ed., AIAA, Reston, VA, 2002, pp. 99–103.

[7] Seidelmann, P. K. (ed.), *Explanatory Supplement to the Astronomical Almanac*, Univ. Science Books, Mill Valley, CA, 1992, pp. 704–711.

[8] Villac, B. F., and Scheeres, D. J., "Escaping Trajectories in the Hill Three-Body Problem and Applications," *Journal of Guidance, Control, and Dynamics*, Vol. 26, No. 2, 2002, pp. 224–232.